Dossier

This paper is a part of the hereunder thematic dossier published in OGST Journal, Vol. 67, No. 6, pp. 883-1039 and available online here

Cet article fait partie du dossier thématique ci-dessous publié dans la revue OGST, Vol. 67, n°6, pp. 883-1039 et téléchargeable ici

DOSSIER Edited by/Sous la direction de : **B. Bazin**

Challenges and New Approaches in EOR

Défis et nouvelles approches en EOR

Oil & Gas Science and Technology – Rev. IFP Energies nouvelles, Vol. 67 (2012), No. 6, pp. 883-1039

IFP Energies nouvelles

Oil & Gas Science and Technology – Rev. IFP Energies nouvelles, Vol. 67 (2012), No. 6, pp. 999-1018

DOI: 10.2516/ogst/2012015

Dossier
Challenges and New Approaches in EOR
Défis et nouvelles approches en EOR

Analysis of Heavy Oil Recovery by Thermal EOR in a Meander Belt: From Geological to Reservoir Modeling

R. Deschamps*, N. Guy, C. Preux and O. Lerat

1 IFP Energies nouvelles, 1-4 avenue de Bois-Préau, 92852 Rueil-Malmaison - France
e-mail: remy.deschamps@ifpen.fr - nicolas.guy@ifpen.fr - christophe.preux@ifpen.fr - olivier.lerat@ifpen.fr

* Corresponding author

Résumé — Analyse de la récupération d'huile lourde par procédé thermique dans une barre de méandre : du modèle géologique à la modélisation de réservoir — Ce travail vise à évaluer l'impact des hétérogénéités d'un réservoir pétrolier sur la récupération d'huiles lourdes par le processus de *Steam Assisted Gravity Drainage* (SAGD) en utilisant des modèles numériques appliqués à un modèle réservoir analogue d'un réservoir type barre de méandre. Ces modèles sont obtenus par un *upscaling* plus ou moins important du modèle géologique.

Les barres de méandre sont constituées de dépôts de point bars, caractérisés par une architecture intérieure complexe en 3-D, avec différentes échelles d'hétérogénéités, dont la taille et la distribution dépend du processus de dépôt.

Basé sur la description d'affleurement de barres de méandre analogues aux champs d'huiles lourdes canadiens, ce travail inclus : 1) la construction d'un modèle réservoir statique de référence basé sur une description très fine des affleurements du point de vue de l'architecture des dépôts et des hétérogénéités de réservoir, 2) l'*upscaling* de la grille à différents degrés afin d'évaluer l'impact de l'*upscaling* sur la distribution des hétérogénéités dans le réservoir, 3) les simulations SAGD en utilisant un doublet horizontal (puits injecteur de vapeur et puits producteur) à travers la barre de méandre, pour évaluer l'impact de l'*upscaling* et des hétérogénéités de réservoir sur la production d'huiles lourdes.

L'impact des hétérogénéités de réservoir sur les résultats de simulation est évalué pour plusieurs degrés d'*upscaling*. Les résultats montrent que la distribution des hétérogénéités de réservoir a un impact sur l'écoulement de l'huile à différents stades de production. Sur le modèle fin de référence, les hétérogénéités de petite taille ont un impact sur le développement de la chambre de vapeur et sur l'écoulement dans le voisinage des puits au début du processus d'injection de vapeur, alors que les hétérogénéités de grande échelle influencent fortement la récupération d'huile tout au long de la production, réduisant l'efficacité du drainage dans le réservoir. Sur les grilles plus grossières, l'effet des hétérogénéités de petite taille peut être affaibli, selon le degré d'*upscaling*. L'effet géomécanique n'est pas pris en compte dans ce travail, le but étant d'évaluer l'impact des hétérogénéités de réservoir sur la récupération d'huile lourde.

La performance du SAGD est clairement liée au développement de la chambre de vapeur, qui dépend du degré d'hétérogénéités dans le réservoir. Les étapes de simulations et l'étude de sensibilité sur le degré d'*upscaling* utilisé contribuent à mieux restituer la distribution des hétérogénéités de réservoir. L'impact négatif de ces hétérogénéités pendant la récupération d'huile lourde doit ainsi être quantifié pour contrôler la récupération aux périodes cruciales de production.

Abstract — Analysis of Heavy Oil Recovery by Thermal EOR in a Meander Belt: from Geological to Reservoir Modeling *— The objectives of this work is to assess the impact of reservoir heterogeneities on heavy oil recovery of a reservoir analogue of meander belt through the Steam Assisted Gravity Drainage (SAGD) process by using numerical models. These models are obtained with different scales of upscaling of the geological model.*

Meander belts consist of point bar deposits, characterized by a 3D complex internal architecture, with different scales of heterogeneities, which distribution is associated with the depositional processes.

Based on a 3D outcrop description of a meander belt analogue to the Canadian heavy-oil fields, the approach includes three steps: 1) the construction of a reference static reservoir model based on a very fine description of the outcrops in terms of architecture and geological heterogeneities, 2) upscaling of the grid at different scales using different upscaling factors in order to evaluate their impact on the heterogeneity distribution in the reservoir, 3) reservoir SAGD simulations using horizontal well doublet (steam injector and producer) across the meander belt, so as to assess the impact of upscaling of heterogeneities on heavy oil production.

The impact of heterogeneities on simulation results are evaluated for several upscaling stages. Results show that heterogeneity distribution has an impact on fluid flow at different stages of production. On the fine gridded model, small scale heterogeneities impact the steam chamber development and fluid flow in the wellbore vicinity at the beginning of the steam injection, whereas large scale heterogeneities strongly influence oil recovery during the whole recovery process and lower the efficiency of the reservoir drainage. On coarser grids, the effect of small-scale heterogeneities can be diminished, depending on the upscaling stage. The geomechanical effect is not taken into account in this work, the objective being to assess the impact of heterogeneities on oil recovery.

The performance of SAGD is clearly linked to the steam chamber development, which depends on the degree of heterogeneities present in the reservoir. The simulation workflow and the sensitivity study on the upscaling method contribute to a better restoration of the heterogeneity distribution in the reservoir. The negative effect of these heterogeneities during the oil recovery must thus be quantified in order to monitor the thermal production at crucial periods of the production process.

INTRODUCTION

SAGD will become increasingly important for heavy oil recovery because of the large resources/reserves accessible using this recovery process. Quantitative reservoir characterization of fluvial meandering reservoirs and petrophysical properties are required for uncertainty assessment, well placement and production performance prediction. One of the most famous heavy oil provinces is located in Alberta (Canada), where SAGD processes are widely used to recover heavy oil from meandering fluvial reservoirs (*e.g.* Mc Murray Formation, Mannville Group, Aptian, Lower Cretaceous).

Characterization and modeling of fluvial reservoirs are straight forward because of the various scales of heterogeneity that exist between and within fluvial deposits (Jackson, 1977; Miall, 1988; Willis, 1989; Sharp *et al*., 2003). The large-scale stratigraphic architecture and small-scale internal heterolithic stratifications of meandering reservoirs are difficult to characterize using subsurface data. Because of the high variability of these deposits, the size of the heterogeneities are commonly smaller than the typical well spacing in developed fields. These depositional units and associated shale drapes can influence reservoir behavior (Swanson, 1993) because they are potential baffles and barriers to fluid flow (Richardson *et al*., 1978; Hartkamp-Bakker and Donselaar, 1993). In addition, internal facies variations, such as the vertical change from trough cross-bedded to ripple-laminated sandstone and silty shales, produce a fining-upward trend in grain-size and a corresponding decrease in porosity and permeability.

To focus on meandering fluvial reservoirs, a very fine gridded reservoir model of a meander belt was built from 3-D outcrop observations of the Scalby Formation (Middle Jurassic Ravenscar Group, U.K.) located in Yorkshire. It had strong similarities with the Mc Murray Fm. heavy oil reservoirs in terms of architecture and facies distribution. This work represents the complex geometries of meandering system reservoirs and accurattely describes the heterogeneity distribution within a meander belt. Several scales of heterogeneities are represented in the fine geological model which has an influence on fluid flow. This fine gridded geological model is taken as a reference model, to be compared with the upscaled models.

The description of thermal fluid flow during the SAGD process in complex reservoirs, such as meander belts, can lead to very very high computation time. Therefore, to describe the steam chamber growth in a reservoir that contains both small and large-scale heterogeneities, the construction of a very fine geological model is required. Upscaling is commonly used to reduce the grid size but it can lead to an over simplified description of the steam chamber growth.

In this paper, simulations describing heavy oil production usingy SAGD process were carried out on upscaled models

that are based on a very fine geological model of a meander belt. The geological model was upscaled along the well pair direction taking into consideration several upscaling factors. No geomechanical simulations were performed as we only looked at the effect of upscaling on the development of the steam chamber. The upscaling was performed using CobraFlow™ while the SAGD reservoir simulations were performed using PumaFlow™. The results were analysed to see if the upscaling factor influences the description of the heterogeneities, a central issue in SAGD production (Birell and Putnam, 2000; Robinson *et al*., 2005, Zhang *et al*., 2005; Chen *et al*., 2007; Lerat *et al*., 2010).

1 HETEROGENEITY DISTRIBUTION IN THE MEANDER BELTS

Meandering systems are made up of high sinuosity rivers that migrate through time. The meanders resulting from the lateral migration of the system are formed by erosion of sediments on the outer bank of the river and deposition of these sediments on the inner part of the meander loop. Banks are steep on the outside of the bend, where erosion generally takes place and are gently sloping on the inside where deposition normally occurs. Reservoir sand bodies originating in high-sinuosity channels result from lateral accretion that accompanies progressive development of increasingly sinuous meandering loops. The gradual, lateral accretion of successive units within a single loop results in the development of a point bar *(Fig. 1)*. Subsequent meander-loop cutoff results in isolation of fully developed point bar sands within overbank muds. Internal mud drapes, common within point bar sands, are the result of low flow regime deposition between each flooding events.

1.1 Meander Belt

In terms of reservoir properties, meander belts present a high degree of complexity in terms of the heterogeneity distribution. Different sizes of heterogeneities can be observed in a meandering system, depending on what we are looking at: the meander or the point bar deposits.

At the scale of a meander, studies on present day analogues and exhumed ancient point bar deposits have shown an overall decrease in the sediment grain size downstream in the meander loop. Satellite image analysis on the present day Senegal River meanders (Joseph *et al*., 1995) shows the facies partitionning along the meander loops *(Fig. 2a)*. Other present day point bar deposits on the modern Peace River (Canada) have been studied and compared to the Mc Murray Fm. regarding the facies distribution (Smith *et al*., 2009). This study also reports the high variability of the grain size distribution along the meanders. These observations have been illustrated by Willis and Tang (2010) through 3-D process-based numerical models. In this study, we also made a fine description of the meander belt deposits of the Scalby Formation (Middle Jurassic) outcropping in the Yorkshire coast (North-East England).

Changes in shape, position and grain size distribution of the channel beds during river floods, preservation of low-flow

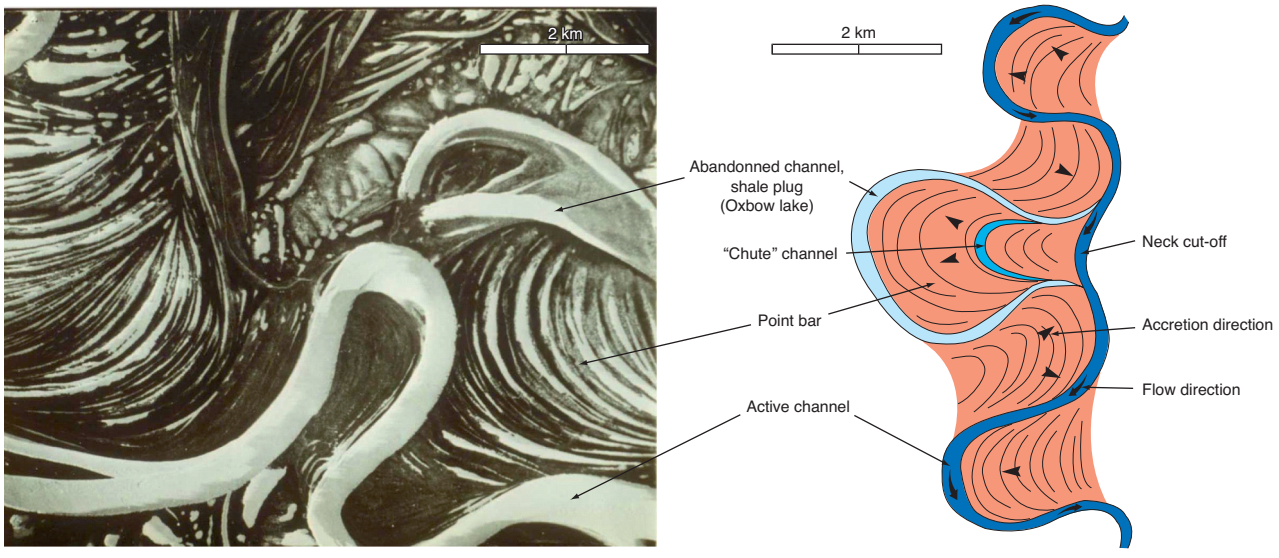

Figure 1

a) Aerial view of a meander belt (Alaska, USA); b) sketch of a meander belt with architectural elements.

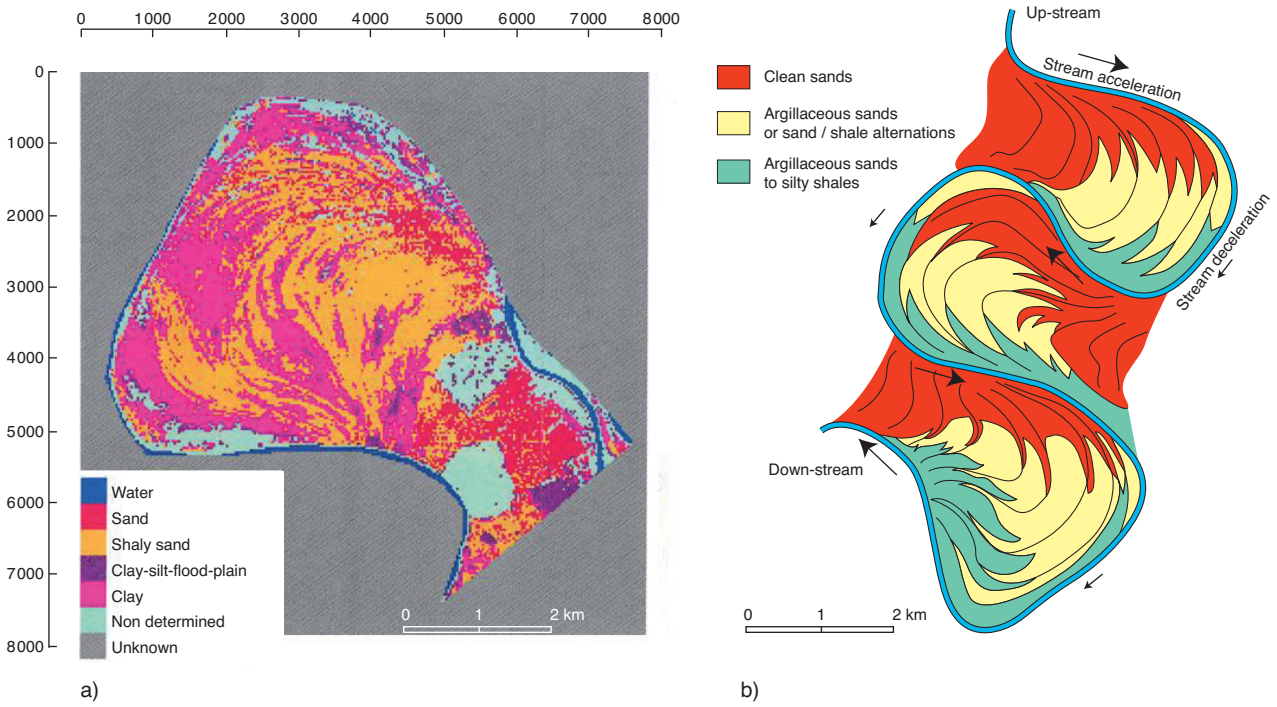

Figure 2

Facies distribution along a meander belt with a) satellite picture analysis of a meander of the Senegal River (Joseph *et al.*, 1995); b) schematic interpretation of the facies distribution in a meander belt.

drapes and abandonment of the channel segments influence the distribution of heterogeneities and consequently the fluid flow patterns through the meander belt sandstones.

This facies partitionning is explained by variations of the fluvial stream velocity along the loop. The coarser material (medium grained sandstones) with the best reservoir properties is thus deposited upstream in the meandering loop, where the current velocity reaches its maximum, whereas the finer grains (fine-grained argillaceous sandstones to silty material) are deposited downstream when the current velocity decreases downstream in the outside of the loop *(Fig. 2b)*.

1.2 Point Bar

Point bar deposits are made up of lateral accretion sets dipping towards the channel axis, which were deposited during the channel migration and channel plugs filled with shales and silts during the channel abandonment *(Fig. 3)*.

Firstly, the thickest and coarsest-grained sediment accumulations are deposited near a channel bend apex. There is a higher accumulation of fine-grained sediments downstream from the channel bar, with an overall shaliness increase vertically and in the direction of the accretion *(Fig. 3)*. In addition, internal facies variations, such as the vertical changes from trough cross-bedded to ripple-laminated sandstone, produce a fining-upward trend in grain size and a corresponding decrease in porosity and permeability.

Shale plugs deposited during the channel abandonment form large heterogeneity all along the meander and can reach several meters in thickness. They may form big permeability barriers at the scale of a meander.

Chute channel plugs also form shaly to silty heterogeneities, which correspond to the decantation of the finer sediments in suspension, filling the low reliefs of the scroll bars during flooding. They may reach up to a meter in thickness and may be found all along the meander.

At smaller scale, shale drapes deposited on individual beds during low flows are preserved mostly on downstream-dipping surfaces in finer-grained bar-top deposits. Shale drapes thickness can reach few tens of centimeters and separate the sandy accretion bars forming reservoir bodies. Extensive finer-grained deposits also accumulate in concave-bank areas in the lee of point bars when meanders migrate downstream. The coarsest deposits occur as elongate bodies parallel to the channel belt axis when channel bends migrate. These depositional units and associated shale drapes can influence reservoir behavior (Swanson, 1993) because they are potential baffles and barriers to fluid flow (Richardson *et al.*, 1978; Hartkamp-Bakker and Donselaar, 1993).

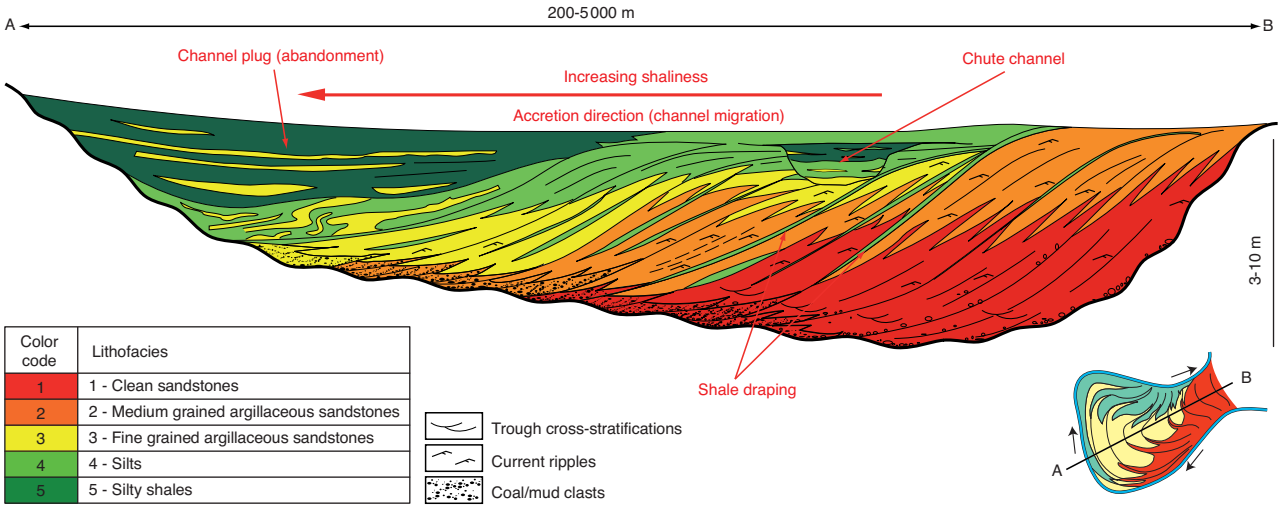

Figure 3

Schematic cross-section in a point bar, with facies spatial organisation and evolution.

The main heterogeneity characteristics commonly described within meandering river deposits observed in the Scalby Formation meander belt (*e.g.* point bar deposits) are summurized in Table 1.

Point bar reservoirs have complex internal architecture and properties (Barton, 1994), with different scales of heterogeneities (channel plugs, shale draping on accretion surfaces) and different directions of heterogeneities (horizontally with increasing shaliness towards the external part of the meander, vertically with the finning upward channel fill succession and obliquely with the shale draping the lateral accretion surfaces along the meander loop). Shale commonly affects flow behavior significantly (Willis and White, 2000), altering vertical permeability (Begg and King, 1985), sweep efficiency and breakthrough time (Jackson and Muggeridge, 2000) and upscaled multiphase flow properties. In the subsurface, the spatial distribution of shale is difficult to infer because the spacing of wells (hundreds to thousands of meters) is typically greater than shale dimensions. Fine outcrop description of meanders is thus crucial to assess reservoir geometry and heterogeneity distribution in 3-D and can be used as an input for geological modeling.

TABLE 1

Reservoir heterogeneity characteristics within the Scalby Formation meander belt

Heterogeneity type	Lithology/depositionnal process	Scale	Heterogeneity dimensions		Extent/continuity	Dominant lithofacies
			Width	Thickness		
Oxbow lake (channel plug)	Shales and silts; vertical accretion processes, suspension, shale decantation in the paleo-river bed when the river cuts its own banks and isolate the meander	Large scale (meander belt to point bar scale)	30-50 m, active paleo-channel width	1-5 m	Hundreds of meters all along the meander bend	Lithofacies 5
Chute channel	Shales and silts; vertical accretion processes suspension, shale decantation in the scroll bar low reliefs after floods	Intermediate to small scale (point bar scale)	1-5 m	0.5-2 m	Hundreds of meters all along the meander bend	Lithofacies 4 and 5
Shale draping	Shales and siltstones; vertical accretion processes, suspension of fine particles during low flow periods (between floods)	Small scale (point bar to laminate sale)	Few meters, thinning towards the toe of the accretion sets	Few mm to 70 cm	Tens to hundred meters in the paleoflow direction. Few meters downward, tend to pinch at the toe of the accretion sets	Lithofacies 4 and 5

2 CONSTRUCTION OF THE GEOLOGICAL MODEL

Outcrop analogues are commonly used to obtain dimensional statistics of fluvial sandstone and shale bodies for 3-D modeling of similar petroleum reservoirs. In most of the cases, outcrops provide 2-D data to assess the reservoir architecture. In this study, plan view dimensions and morphology of the point bar sand bodies are described from outcrops located on the Yorkshire coast in U.K. close to the town of Scarborough (Scalby Formation, Ravenscar Group, Middle Jurassic). These series have been deposited in the Cleveland basin, which was limited northeastward by the Pennine High and southward by the Market Weighton Block. In this area, the Cleveland basin formed a slowly subsiding trough, which trapped siliciclastics sediments. A deltaic system prograded gradually from the North to the Southeast and it is supposed that a connection with the open marine environments existed in the East (Eschard *et al*., 1991).

At this location, meander belts crops out on a strand plain in plane view, with an equivalent cropping out on a cliff few kilometers South. Both the outcrop analogue (Scalby Formation) and subsurface reservoir (Mc Murray Formation) are interpreted to have some marine and/or tidal influence (*e.g*. Pemberton *et al*., 1982; Smith, 1988; Eschard *et al*., 1991; Alexander, 1992), at least locally. This may make more heterogeneous than conventional meandering fluvial deposits. This analogy is discussed below in Section 2.1.

High resolution geologic modeling of outcrops is useful to identify the types and scales of lithologic and petrophysical heterogeneities that affect fluid flow behavior. Many studies have already explored geological modeling of various scales of heterogeneities within fluvial reservoirs (process based, deterministic and stochastic). Many of these studies investigate stratigraphic architecture (sand and shale body dimensions and distribution) and reservoir connectivity and heterogeneity assessment at the reservoir scale (Richardson *et al*., 1978). Other studies focused on the potential effect on fluid flow of internal sand bodies and shale heterogeneities (Hartkamp-Bakker and Donselaar, 1993; Lerat *et al*., 2010).

Using stochastic methods, 2-D and 3-D modeling of point bar deposits in the Middle Jurassic Scalby Formation (Yorkshire, UK) were carried out to evaluate small-scale heterogeneities within the point bar deposits. Sedimentological description collected from outcrops were used to build the fine reference model and served as constraints for geological modeling.

2.1 Analogy with Subsurface Mc Murray Formation

The Mc Murray formation, the main bitumen-bearing zone in the Athabasca deposit (Eastern Alberta, Canada), is a member of the Mannville group (Lower Cretaceous). The Mc Murray Formation is characterized by highly heterogeneous strata that have been attributed to fluvial, estuarine and/or deltaic depositional settings (Flach and Mossop, 1985; Crerar and Arnott, 2007). The Mc Murray Formation (Fm.) is a heterogeneous amalgamation of a variety of sedimentological elements such as point bars that evolved through lateral channel migration, point bars developed through downstream translation, counter point bars, sandstone-filled channels and abandoned channels or oxbows. Point bar of fluvio-estuarine channels are made up of fine-grained sandstones with ripple bedding alternating with argillaceous sandstone and mud drapes. Bioturbations are abundant at the core scale. The bedding is oblique, forming large bedforms several meters thick with a similar dip. The facies is classically called Inclined Heterolithic Stratification (IHS). The facies association is extremely heterolithic, the sand/shale ratio usually being relatively low.

The Scalby Formation is also interpreted as a fluvio-deltaic series (Eschard *et al*., 1991), which can be divided into two main members. It is interpreted as a incised valley-fill complex created during the Lowstand System Tracts (LST), and filled by a deltaic aggradational series during the subsequent Transgressive System Tracts (TST). The meander belt deposits corresponding to the valley fill consists of fine to medium-grained clean to argillaceous sandstones. The meander belt is made up of stacked point bars and clay plugs, deposited in a fluvial – dominated environment. However, abundant clay drapes on the accretion surfaces, bioturbation and reverse ripples indicate a tidal influence.

Point bar deposits of both Scalby Fm. and Mc Murray Fm. correspond to tidally-influenced fluvial deposits, which makes the heterogeneity pattern comparable for these two systems (*e.g*. mud accumulation during channel abandonment, mud drapes along accretion surfaces that are interfingered into cleaner sands, floodplain deposits on top of the point bar; reactivation surfaces typically associated with mud-clast deposits; and mud-clast breccias accumulated at the base of the channel).

However, there are some limitations in the similarities between the Scalby Fm. and the Mc Murray Fm. The dimensions of the Mc Murray point bars are larger than the Scalby Fm. point bars. Musial *et al*. (2011) describe a meander loop width ranging between 4 and 8 km, with a point bar thickness of 30 m. The point bars of the Scalby Fm. are much smaller: their width is estimated between 500 m and 1 km and their thicknesses are less than 10 m. Consequently, the size of the heterogeneities is overall greater in the Mc Murray point bar deposits than in the Scalby Fm. The size of the "small-scale" heterogeneities is a critical factor for both geological modeling and thermal modeling. A high resolution geological model based on the Scalby Fm. outcrops was built to take these "small-scale" heterogeneities into account.

2.2 Outcrop Description and Interpretation

The point bar deposits used for the geological model crop out in South Bay cliffs, in the southern part of Scarborough

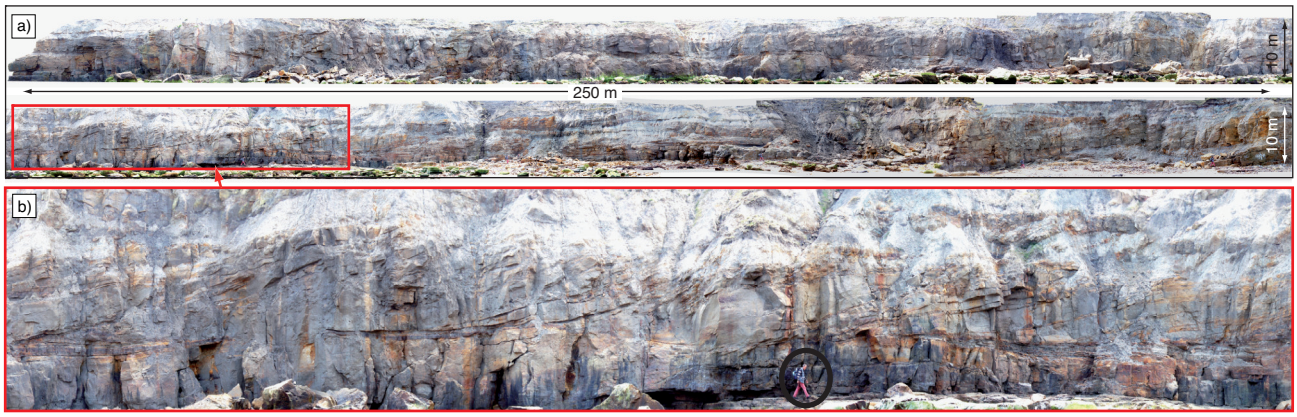

Figure 4

a) Photopanel of the South Bay cliff meander belt outcrop; b) detail picture of a point bar in South Bay cliff outcrop.

(Yorkshire, U.K.). The South Bay cliff displays a meander belt filling an incised valley and the same unit can be observed in plane view on the seashore 5 km to the north.

In South Bay, the meander belts directly overlie shaly marine sediments, with an irregular erosionnal surface at the base corresponding to the base of the incised valley. The incised valley fill forms a very heterogeneous sand sheet, 15 m thick, made up of fine to medium-grained argillaceous sandstones and shales *(Fig. 4a, b)*. It consists of two stacked meander belts separated by an erosional surface. The width of the meander-belt cannot be estimated because it encompasses the outcrop size. The southern and northern limits of the meander belt can be seen on the South Bay site and the width of the meander-belt is around 1 km.

The meander belt deposits consist of point bars, chute channels and channel plugs ("oxbow" plugs) and the system is sealed by shaly coastal plain deposits:

– the point bars are made up of medium-grained trough cross stratifications *(Fig. 5a)* and fine-grained ripple-laminated sandstones *(Fig. 5b)*, organized in a finning upward sequence, with a shaliness increasing in the uppermost part. Scour surfaces with mud clasts and coal clasts are commonly found at the base of the meander belts. The large-scale oblique stratifications are observed (equivalent of Inclined Heterolithic Stratifications, IHS), forming sets of 2 to 3 m in thickness *(Fig. 5c)*. Each oblique set is tens of centimeters thick and the dip of those sets ranges from 10 to 20°. These inclined stratifications are forming the lateral accretion sets of the point bars, with shale drapping centimeter to decimeter thick on top, developing towards the top of the accretion surface. Slump scars can also affect the lateral accretion sets. They correspond to the channel bank collapse towards the channel axis. Each meander belt observed on the South Bay cliff is respectively 3 m and 8 m thick. The lowermost meander belt is erosionally truncated by the uppermost one;
– chute channels are frequently observed incising the top of the point bars. Chute channels are formed during floodings as the channels start to cut the meander. They are filled by silty shales *(Fig. 1, 2)*;
– the "oxbow" plugs are 40 m wide and made up of silty shales and argillaceous sandstones, locally deformed by slumping. Coal layers are also locally present *(Fig. 5d)*. The channel plugs correspond to the filling in of abandonned channel loops when the stream cuts its own meander. Mud and organic material is then accumulated in the abandonned meander loop;
– the coastal plain deposits consist of shales and silty shales with local sandy crevasse splay deposits. This shaly interval caps the meander belts and acts as a seal to the reservoir.

The meander belt outcropping on the South Bay cliff also crops out in the strand plain along the shoreline 5 km northward. This meander belt is made up of several nested point bars eroding each other, associated with shale plugs. The meander belt geometry can thus be described and interpreted in 3-D. The radius of point bars can reach more than 400 m, with an asymetrical radius of curvature and their thickness can reach 8 m.

The outcrops are interpreted in terms of lithofacies, which were directly used for geostatistical simulations *(Fig. 6)*.

2.3 Definition of Lithofacies

The lithofacies are defined as being based on both grain size and shale content. Five lithofacies were interpreted from outcrop observations:

– lithofacies 1: clean medium to coarse-grained, massive to trough cross-bedded sandstone facies, mostly present at

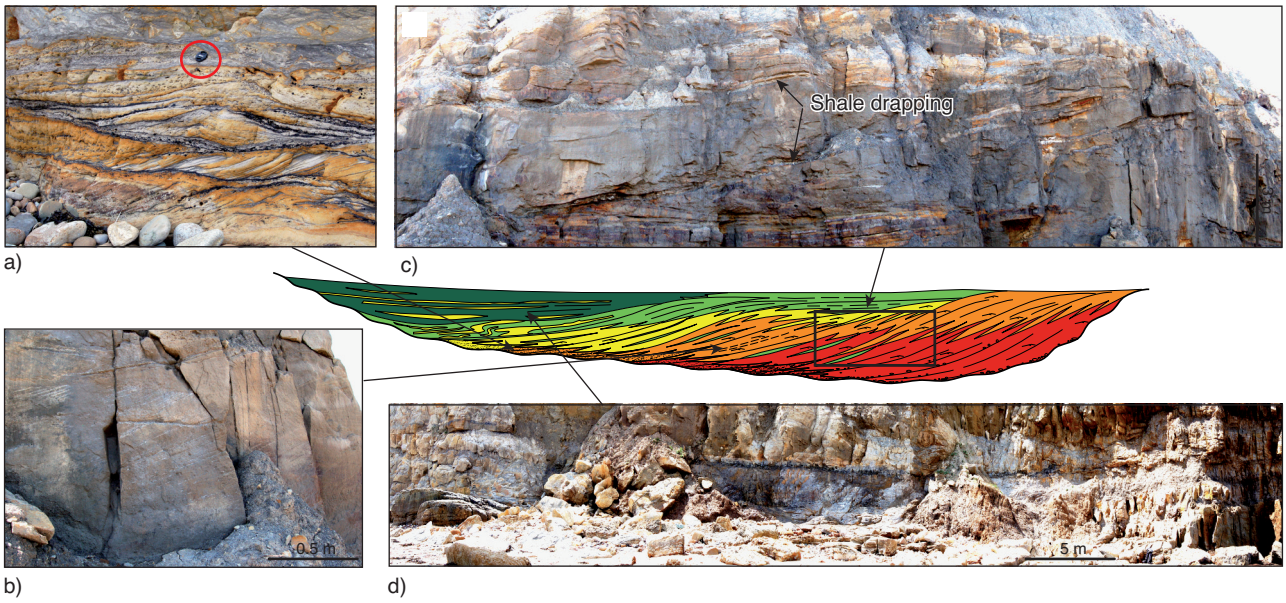

Figure 5

Main facies associations of a point bar. a) Coarse grained sandstones with trough cross-stratifications at the base of the meandering channel; b) medium grained sandstones with rippled inclined stratifications; c) lateral accretion sets of a point bar with shale draping on top of the sets; d) channel plug filled with silty shales and coal deposits.

the base of the lateral accretion sets and in the most internal parts of the meander loops;

- lithofacies 2: medium-grained slightly argillaceous sandstone with ripple lamination facies. This lithofacies is mostly associated with the middle part of the lateral accretion sets;
- lithofacies 3: fine-grained shaly sandstone with fine shaly laminations and current ripples. It occurs mostly in the uppermost part of the lateral accretion sets as well as at the bottom of the chute channels and channel plugs;
- lithofacies 4: silty shales facies. This lithofacies is associated with the main heterolithic facies associations of the reservoir, represented by the shale drapping on the lateral accretion bars and the chute channel and channel plug infills;
- lithofacies 5: shaly facies related to channel abandonment mud plugs, floodplain or coastal plain shales.

2.4 Litho-Units Definition

The litho-unit definition is a crucial factor in reservoir modeling. It corresponds to the reservoir units having geological characteristics that need to be simulated with proper geostatistical parameters (point bar deposits, floodplain interval, channel plugs...). Litho-units are delimited by two surfaces. The lithostratigraphic units correspond to intervals characterized by their depositional environment and related reservoir architecture. These units are simulated independantly with appropriated simulation parameters defined according to their geometry and depositionnal process.

Ten lithostratigraphic units are identified in the South Bay meander belts interval *(Fig. 7a)*:

- units 1, 2 and 6: these units correspond to medium to fine-grained sandstones and sand/shale alternations interpreted as point bar deposits with lateral accretion sets. Despite the complex heterogeneity pattern, these units are the main reservoir units of the meander belt system. The main lithofacies present in these units are Lithofacies 1, 2, 3 for the reservoir bodies and lithofacies 4 that corresponds to shale draping the accretion sets;
- units 3, 4 and 7: they are made up of shales and fine grained shaly sandstones and they correspond to channel plugs. The associated lithofacies are Lithofacies 4 and 5;
- units 5, 8 and 9: these units are made up of medium to fine grained shaly sandstones with abundant shale drapes and heterolithics. They correspond to chute channels infills, bounded by erosionnal surfaces at the bottom cutting into the point bar deposits. They are characterized by Lithofacies 2, 3 and 4;
- unit 10: this uppermost unit corresponds to a discontinuous shale interval, deposited above the meander belts It is interpreted as a coastal plain environment. This unit is not a reservoir. The main lithofacies present in these units are Lithofacies 4 and 5.

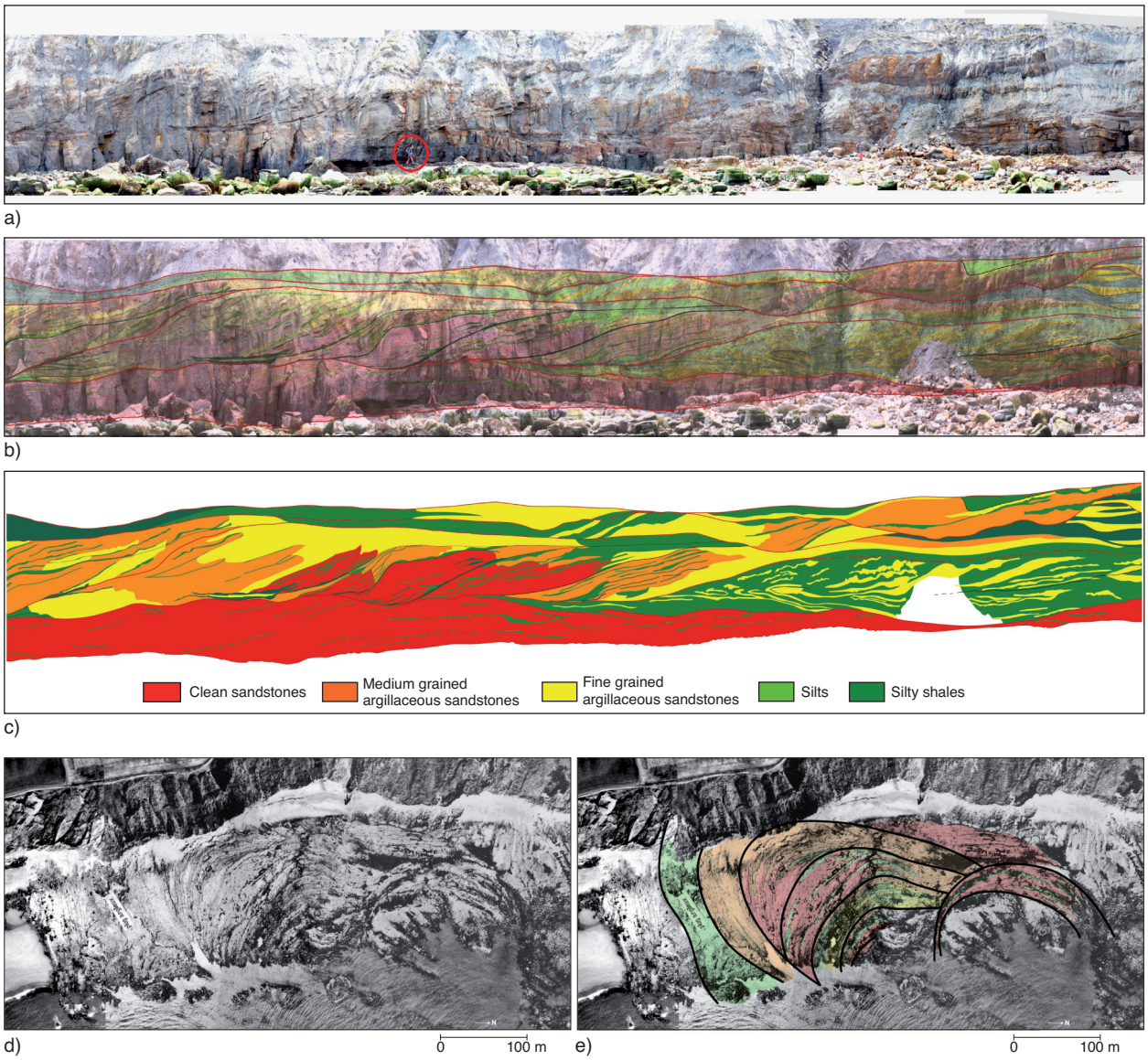

Figure 6

a) Outcrop picture of the meander belt (South Bay cliff); b) linedrawing and facies interpretation of the outcrop picture; c) lithofacies interpretation used as simulation constrains; d) aerial picture of the meander belt outcropping in the strand plain; e) interpretation of the meander belt aerial picture.

2.5 Geostatistical Modeling

The geological grid built for the reservoir zone contains about 3×10^6 cells, using a Cartesian grid with a definition of $2\,m \times 2\,m \times 0.25\,m$. The ten lithostratigraphic units are modeled independently using a stochastic approach, based on the truncated Gaussian method (Galli *et al*., 1994, Le Loch and Galli, 1996, Doligez *et al*., 1999, Eschard *et al*., 2002, Galli *et al*., 2006). The main geostatistical parameters which are used in the truncated Gaussian method are the vertical proportion curves, the matrix of proportions and the variograms, which are all computed from the maps and outcrop descriptions. In the present study, the South bay cliff interpretation and two maps of the meander belts interpreted in terms of lithofacies are used to build the stochastic model (Doligez *et al*., 1999).

2.5.1 Geological Constraints

The constraints used for the geostatistical model directly come from the outcrop interpretations. Using the outcrop

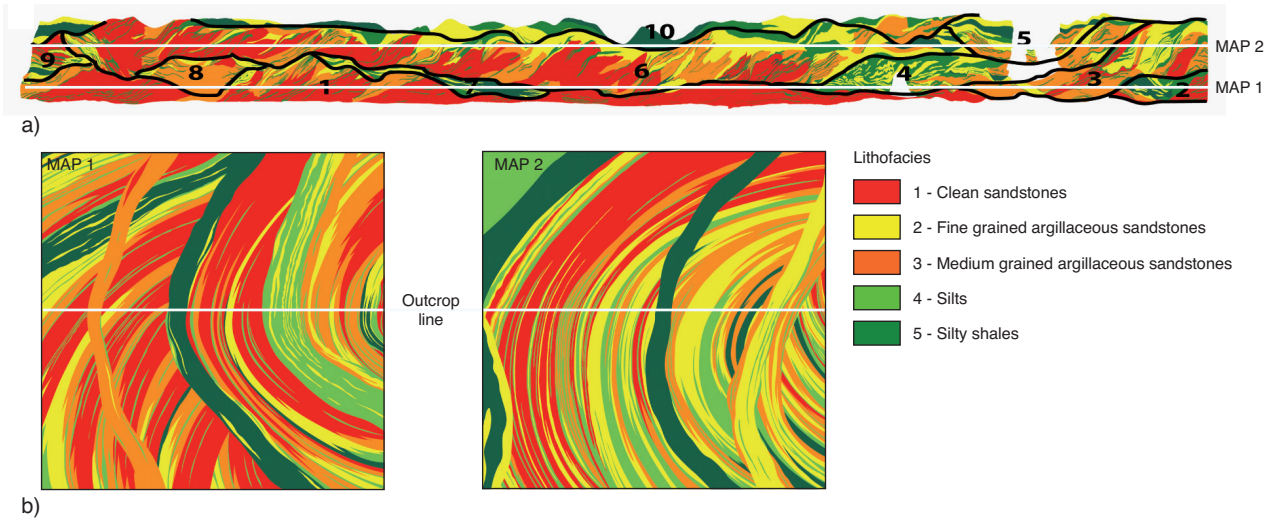

Figure 7

a) Meander belt outcrop interpretation and litho-units definition; b) maps of the meander belt derived from the strand plain outcrops.

interpretation, two maps representing the meander geometry and lithofacies distribution along the meander loops were built to restore the meander belt architecture in 3-D. These maps are interpretations from the 2-D view of the outcrop as shown in Figure 7 and extended laterally to cover the whole model. The distribution of the facies and geometries on these maps are constrained by the strand plain outcrop interpretation. These maps fit the oucrop interpretation and they were drawn with respect to the meander size and curvature observed in the strand plain outcrop. The litho-facies distribution was also extrapolated from the strand plain outcrop observations (horizontal grain size and shaliness evolution along the meander loops) to fit a realistic meander belt facies and architecture. The first map represents the lower meander belt described on the outcrop, the second one the upper meander belt *(Fig.7b)*.

Both maps and the outcrop description were directly used as constraints (hard data, properties painted on the grid) for the geological model.

2.5.2 Geostatistical Parameters

The truncated gaussian method was the geostatistical method used to simulate the ten litho-units, using 3-D variograms dipping towards the direction of accretion for the point bars, and ordinary kriging for channel plugs and coastal plain deposits on top of the meander belts.

The truncated Gaussian method was relevant to simulate most of the reservoir heterogeneities which are homogeneously distributed within the volume of simulation (*e.g.* shale drapping the lateral accretion sets, chute channels filled by shales...). In the truncated Gaussian method, the facies distribution is obtained by truncation of a Gaussian (normal) Random Function. Truncation thresholds depend on the proportions of facies in each litho-unit and on the relationship between the different lithotypes (contacts and transitions). The Gaussian Random Function is stationary but the proportions (hence the thresholds) can vary in space (Beucher *et al*., 1993; Galli *et al*., 1994; Le Loch and Galli, 1996; Doligez *et al*., 2007). This method was applied to litho-units corresponding to point bar deposits (litho-units 1, 2 and 6), and to chute channels heterogeneously filled by sands and shales (litho-units 5, 8 and 9).

Ordinary Kriging method was applied to the litho-units that correspond to shaly channel plugs (litho-units 4 and 7) and to the coastal plain deposits sealing the meander belts (litho-unit 10).

Point bar modeling with a Cartesian grid is quite challenging because of its complex internal architecture. The different directions of sedimentary structures (inclined stratifications in the direction of channel migration) and the curvature of the meander are difficult to model by using "simple" geostatistical parameters.

Variograms are the main parameters used to fill in the grid. The variograms are distance dependent mathematical functions, which characterize the spatial correlation of a given property, or function. These functions are half-average values of the square difference between the observed values at two points separated by a distance h and are calculated along the vertical and two horizontal directions. The experimental variograms are computed for differents groups of lithotypes. It is necessary to define the anisotropy direction and the three ranges.

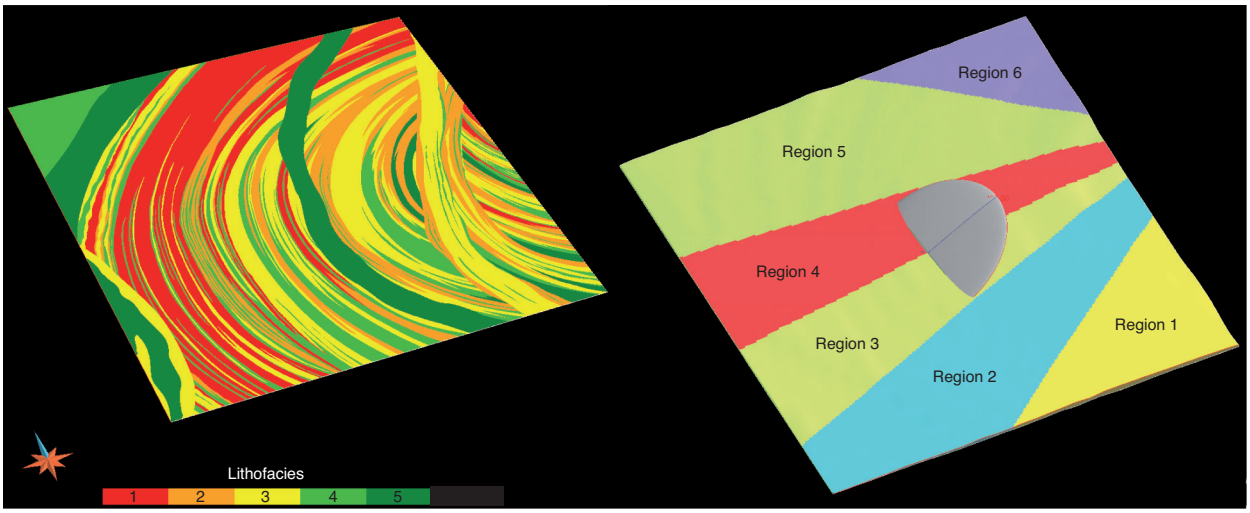

Figure 8

Simulation region definition according to the azimuth of the meandering channel migration (direction of accretion).

The variograms are computed taking into consideration the facies proportions in each litho-unit, computed from both maps and outcrop interpretation that are discretized and assigned as propetries within the grid. Within the IHS litho-units, the variograms are computed along the individual beds to better represent the "small scale" heterogeneities draping the bed sets whose dimensions reach the vertical grid resolution (0.25 m).

The exponential variogram model best fits the experimental variograms. To respect the geometry of the inclined stratifications, 3-D variograms were defined, with a dip of 10 to 20° in the direction of point bar accretion.

The main difficulty was to reproduce the point bar infill along the meander loop, as the direction of point bar accretion changes along a curve corresponding to the loop. To overcome the fact that no direct tools are available to define several variograms along a curve, we defined several regions in each litho-unit according to the azimuth of the accretion direction *(Fig. 8)* and we assigned a variogram to each region with the appropriate azimuth.

2.5.3 Petrophysical Properties

For each litho-facies, single constant value of porosity, horizontal and vertical permeabilities have been attributed. The petrophysical properties used in this model were derived from measurements on core plugs of Hanginstone heavy oil field in Athabasca (Alberta, Canada), in which SAGD processes are used to produce heavy oil in the Mc Murray Formation. The petrophysical properties of each litho-facies are shown in Table 2.

TABLE 2

Reservoir rock properties

	Lithofacies				
	1	2	3	4	5
Porosity (%)	0.35	0.25	0.20	0.05	0.01
Horizontal absolute permeability (mD)	3 000	2 500	2 000	0.5	0.1
Vertical absolute permeability (mD)	2 000	1 300	1 000	0.4	0.01

2.5.4 Simulation Results

The simulation results are displayed for one realization in Figure 9. The high-resolution geological model resulting from the application of the previously described methodology well fit to the conceptual geological model established using the outcrop observations. The large-scale architecture of the meander belt is satisfactorily represented regarding the heterogeneity distribution and the point bars geometries. The meander curvature as well as the heterogeneity distribution along the meander loop is very close to the expected architecture and litho-facies distribution.

The fine-gridded model also allowed the reproduction of the small-scale heterogeneities (*e.g.* shale drapes on the lateral accretion sets) within the point bar deposits, when their thicknesses exceed the grid resolution.

Very fine outcrop descriptions were used to contrain the model. Regions of simulation were defined according to the azimuth of the accretion direction and simulated using 3-D variograms to account for the dip of the sedimentary structures.

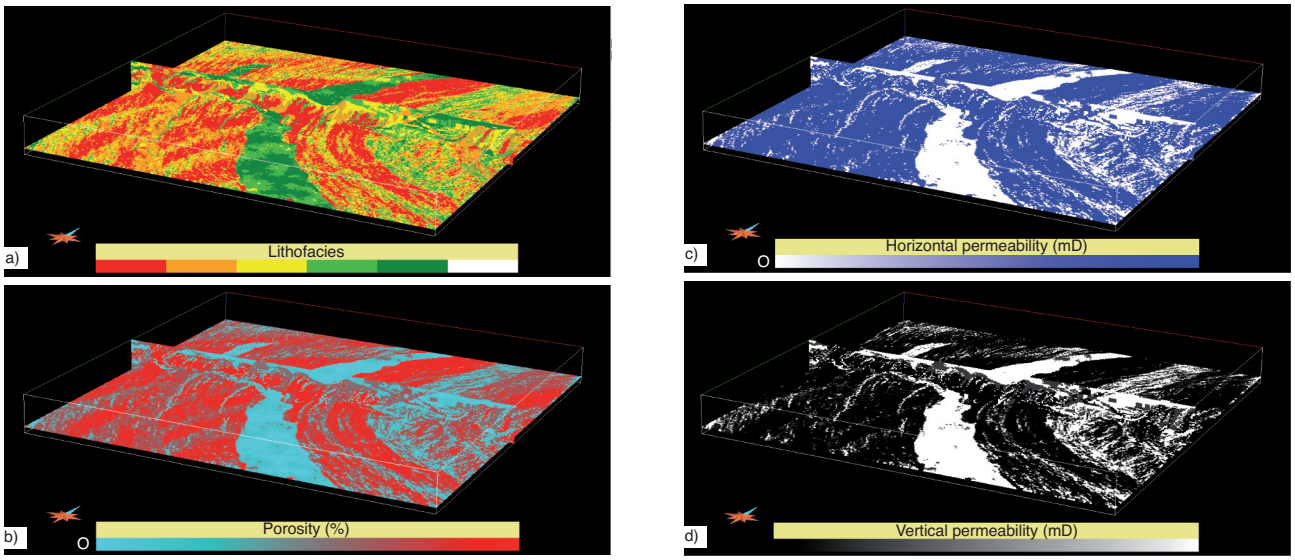

Figure 9

3-D view of the simulation results of the meander belt.
a) Litho-facies; b) porosity; c) horizontal permeability; d) vertical permeability.

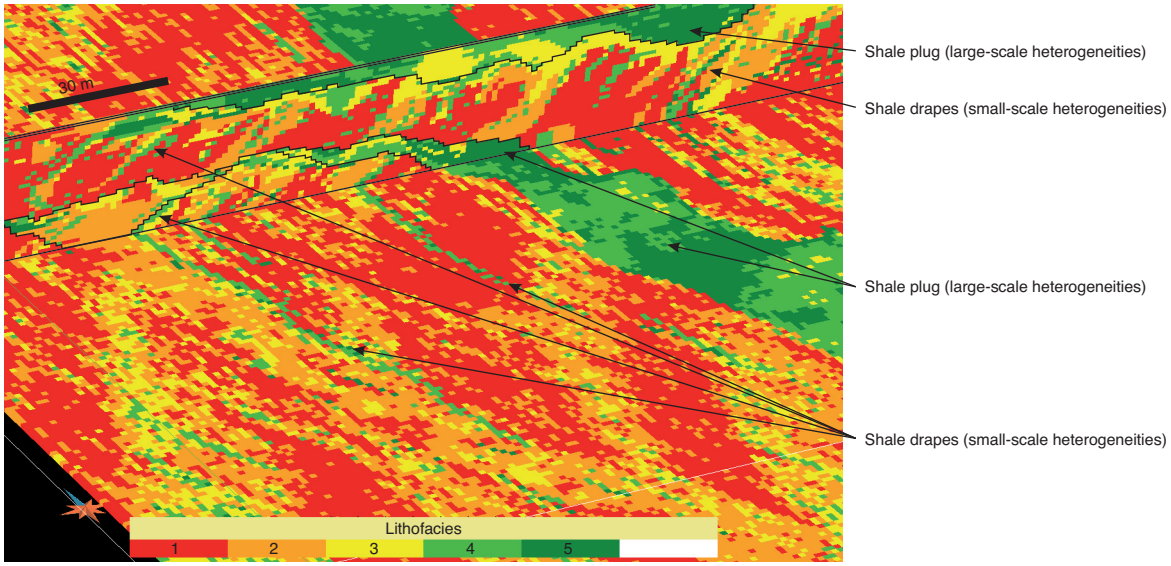

Figure 10

Detailled view of the simulation results showing the different degrees of heterogeneities.

This approach allowed the simulation of the 3-D complex architecture of the meander belts, with a good representation of the different heterogeneity scales *(Tab. 1)*.

The "small-scale" heterogeneities (*e.g.* shale drapes) are realistically represented when their thicknesses are above the vertical grid resolution (25 cm), which is not the case for all the clay drapes described on outcrop. For a drape thickness below the vertical grid resolution (< 25 cm), they are under-represented in the model and not continuous ("speckled" heterogeneity distribution). Even a high-resolution Cartesian grid may struggle to incorporate dipping shale barriers and similar features – these tend to be represented in a "stair-step" fashion which can artificially reduce their continuity *(Fig. 10)*. However, shale drapes more than 25 cm thick are continuously represented in the model along the meander scroll bar and laterally disappear, as shown in Figure 10.

3 UPSCALING OF THE GRID

Upscaling is a procedure that transforms a detailed geological model into a coarse-grid simulation model so that the flow behaviour in the two systems is similar. Upscaling is commonly required because in most of the cases, fine scale flow simulation of high-resolution model induces high computation times. Any upscaling procedure involves two steps:

– gridding to capture the geologic features;
– averaging or estimation of properties, to preserve the local geological details.

Different authors (Renard and De Marsily, 1997; Durlofsky, 2003) have stated the advantages and the limits of different upscaling procedures and despite the numerous upscaling methods reported in the literature, efficient and accurate estimation of effective rock properties of coarse scale from geological data at fine scale remains an active research area. The upscaling procedure to apply will depend on the depositional setting (*e.g.* heterogeneity distribution) and on the type of fluid flow modeling. Over the past decades, the role of reservoir heterogeneities has been investigated both numerically and experimentally.

Many authors who conducted both numerical and experimental work (Joshi and Threlkeld, 1985; Farouq-Ali, 1997; Yang and Butler, 1992) pointed out that the reservoir heterogeneities may strongly influence the steam chamber growth and subsequently the oil recovery. For example, the steam chamber growth has been observed using 4D and crosswell seismic images at the Christina Lake SAGD project (Zhang *et al*., 2007). This study clearly showed that the steam chamber growth was not regular. The authors have associated the irregularities of the steam chamber growth with *in situ* heterogeneities and demonstrated that reservoir heterogeneities is a key issue in SAGD performance evaluation.

In the case of meander belt deposits, we demonstrate the strong anisotropy concerning the heterogeneities distribution. The choice of the upscaling method is thus crucial to keep the maximum of reservoir heterogeneities in the model. In this study, we choosed to place the well in the same direction as the point bar accretion direction. The point bars are oriented perpendicularly to the direction *X*. By upgridding in the direction *X* we better preserve the heterogeneities that are laterally extended. The main flow direction is in the *Y* direction, and the reservoir is strongly heterogeneous in the direction *Z*. Upscaling the grid in directions *Y* and/or *Z* would suppress most of the heterogeneities in the coarse grid. In this study, the grid is upscaled only in the well direction (*X* direction). This choice is also supported by the fact that the steam chamber grows lateraly to the well (directions *Y* and *Z*) and a good description of the steam chamber growth evolution requires a fine grid resolution in those directions.

The Lemouzy method (Lemouzy *et al*., 1993) is built from the Cardwell and Parson bound, was used in this case (Cardwell and Parsons, 1945). The Cardwell and Parsons bound is based on a variational method for the upscaling of permeability. To compute the lower bound in the direction *X*, if we note μ_a^i the arithmetic mean in *i* direction, μ_h^j the harmonic mean in *j* direction and k_x the permeability in *X* direction of the fine cell, according to Cardwell and Parson, the lower bound is written:

$$K_x^{\min} = \mu_a^z(\mu_a^y(\mu_h^x(k_x)))$$

To compute the upper bound, we have:

$$K_x^{\max} = \mu_h^x(\mu_a^z(\mu_a^y(k_x)))$$

Lemouzy *et al*. (1993) adapted the Cardwell and Parsons mean for a 3-D computation. They applied the same method in all directions to obtain:

$$K_x^{\text{Lemouzy}} = \sqrt[6]{\left(K_x^{\min}\right)^2 \left(K_x^{\max}\right)^2 K_x^3 K_x^4}$$

with:

$$K_x^3 = \mu_a^y(\mu_h^x(\mu_a^z(k_x)))$$

and:

$$K_x^4 = \mu_a^z(\mu_h^x(\mu_a^y(k_x)))$$

In our test case, the geological model is a carthesian grid with 3×10^6 cells. For both upscaling tests and SAGD simulations, we extracted a portion of the original geological model, which includes 210 × 75 × 45 cells, to reduce the computation time. We tested different upgriding in the direction *X* (along the well direction). Different upscaling factors (Preux, 2011) were choosen in the well direction (aggregation of 2, 3, 5, 6, 10, 15, 21 cells). Preux (2011) defines the upscaling factor by:

$$UF = \frac{N_c}{N_f}$$

where N_f and N_c are the number of cells in the stratigraphic/reservoir grid.

The upscaling extended parameter was computed (Preux, 2011; Qi and Hesketh, 2004). This parameter is defined by the following formula:

$$UE = 1 - \frac{\ln\left(N_c\right)}{\ln\left(N_f\right)}$$

The results are reported in Table 3.

4 SAGD DYNAMIC MODELING

In the SAGD process, two parallel horizontal oil wells are drilled in the formation, one about 4 to 6 metres above the other *(Fig. 11a)*. The upper well injects steam and the lower one collects the heated crude oil or bitumen that flows out of the formation, along with any water from the condensation of injected steam. The basis of the process is that the injected steam forms a "steam chamber" that increases vertically and horizontally in the formation *(Fig. 11b)*. The heat from the

TABLE 3

Upscaling factor

Nx	Ny	Nz	Total nb. of cells	Upscaling factor
105	75	45	354 375	0.5 (upscaling ×2)
70	75	45	236 250	0.33 (upscaling ×3)
42	75	45	141 750	0.2 (upscaling ×5)
35	75	45	118 121	0.167 (upscaling ×6)
21	75	45	70 875	0.1 (upscaling ×10)
14	75	45	47 250	0.0667 (upscaling ×15)
10	75	45	33 750	0.04761 (upscaling ×21)

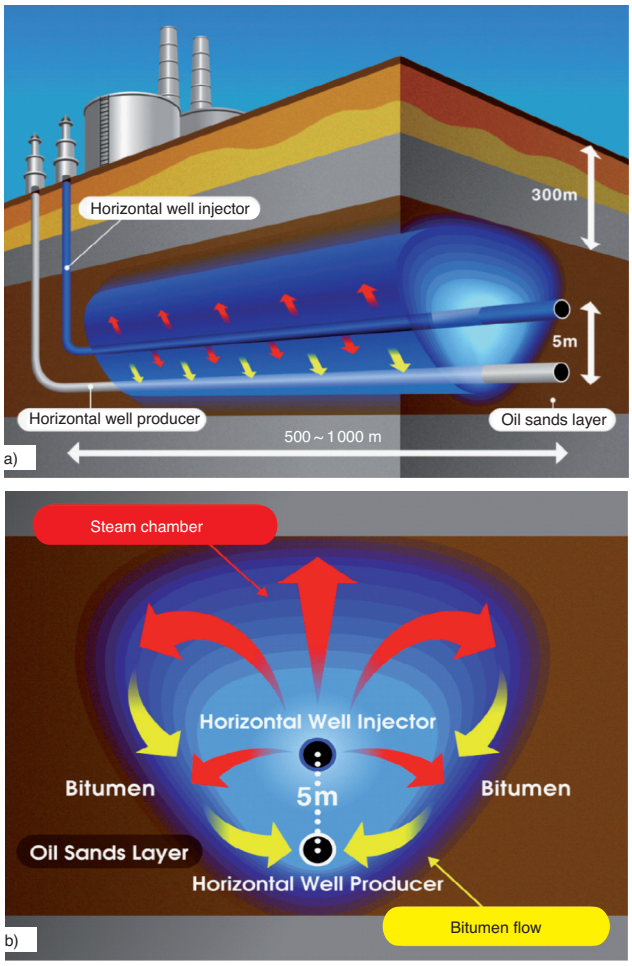

Figure 11

a) Well devices (injector and producer) used in a SAGD process; b) sketch showing the steam chamber during steam injection. Images courtesy of Jacos.

steam reduces the viscosity of the heavy crude oil or bitumen allowing it to flow down into the lower wellbore.

For all the studied cases, the numerical modeling aims at describing heavy oil recovery by a SAGD process. The simulations were performed using the finite volume based reservoir simulator. In the present case, a dead-oil behaviour is considered. This simplification is performed because it commonly assumed that the dissolved gas fraction can be neglected in Canadian heavy oil fields.

In this section, the framework of the simulation is described by adding parameters and by describing, the boundary conditions and the way injectors and producers are controlled. The simulations only concern a small part of the geological model and we focused on the beginning of the injection period, before the steam chamber reaches the reservoir limits. The reservoir-simulated domain is rectangular with its dimensions in the *X*, *Y* and *Z* directions respectively equal to 420 m, 150 m and 18 m. The well pair is located along the *X*-axis and in the middle of the model along the *Y*-axis. For all the studied cases, the distance between the two wells is 6 m. The producer (located under the injector) is 3 m above the base of the reservoir. Both the injector and the producer lengths are equal to the reservoir length in the direction *X*.

4.1 Other Parameters

The reservoir parameters used for SAGD simulation come from the Hangingstone heavy oil field (Canada). The initial conditions are realistic and consistant with the depth of the top of the reservoir, which is 250 m. The initial pressure and temperature are equal to 24 bar at the top of the reservoir and 10°C respectively. The initial oil saturation is equal to 0.85. The oil properties are summarized in Table 4.

The irreducible water saturation is 0.15; the residual oil saturation to waterflood is 0.20 and the residual oil saturation to steamflood is 0.10.

In order to simplify the analysis and for all the considered cases, the geomechanical coupling was not performed. However, the rock compressibility is considered in the reservoir simulator. For all the litho-facies, the rock compressibility is set at 10^{-3} bar^{-1}. The thermal properties of the rocks are also homegeneous in the reservoir. The rock thermal conductivity is 2.0 W/(m.°C) and the heat capacity is 1.7 J/(cm^3.°C). It is however well known that the geomechanical effects of temperature and pressure can alter the behaviour of reservoir materials. In this study, we focused on upscaling.

TABLE 4

Oil properties

Oil properties	Values
Oil density ($g.cm^{-3}$)	1.008
Oil viscosity at reservoir conditions (cP)	1.8×10^6
Oil viscosity at 264°C (cP)	2.74
Oil compressibility (bar^{-1})	2.17×10^{-4}
Oil thermal expansion coefficient ($°C^{-1}$)	8.5×10^{-4}

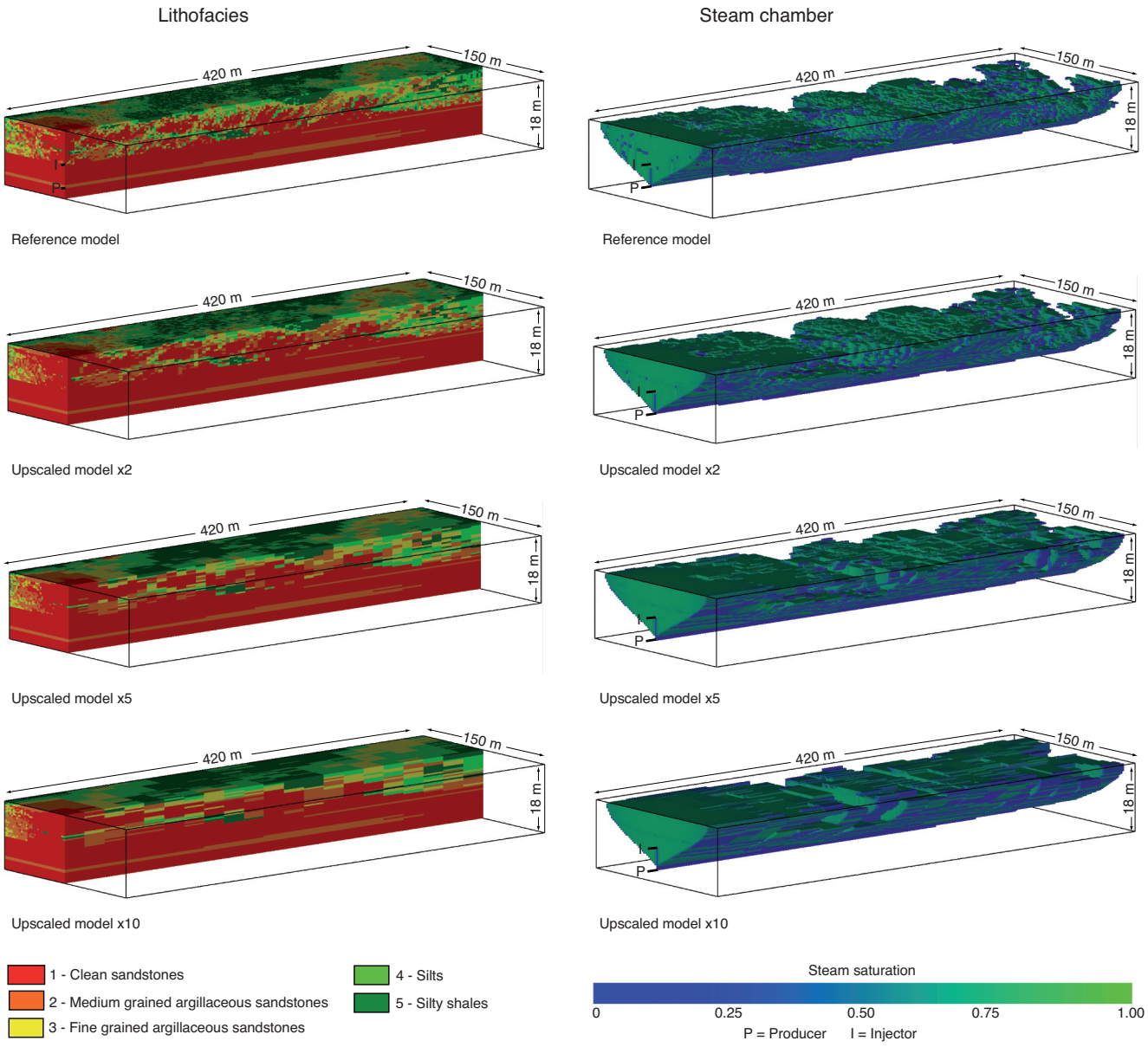

Figure 12

Lithofacies distribution and steam chamber development after 2 000 days in the different upscaled models, compared to the reference model.

4.2 Boundary Conditions and Wells

For all the studied cases, sideburden rocks are not modeled. This assumption corresponds to the fact that in a SAGD process, it is common to use several pairs of wells that are parallel and equidistant to optimize production rates. In the model associated with the reservoir simulator, fluids or heat cannot flow through the lateral boundaries. Fluids cannot flow through the upper and lower boundaries. Nevertheless, heat losses by conduction through upper and lower boundaries were taken into account by using one-dimensional modeling of the overburden and underburden oriented in the vertical direction. The overburden and the underburden models are not represented in the figures and they have a width of respectively 50 m and 30 m. These burdens are homogeneous; they are considered as being made up of rocks that have a thermal conductivity of 2.3 W/(m.°C) and a heat capacity of 2.0 J/(cm^3.°C).

The simulations were performed over 2 000 days. The first 120 days were spent in pre-heating. The steam injection started at the end of the pre-heating phase with a maximal pressure set to 50 bar and the steam injection temperature is about 260°C. The production-well minimal pressure was set of 5 bar and the production rate was automated in order to keep the production well temperature between 20°C and 35°C lower than the injection-well temperature. When the difference between the temperature of the producer and the temperature of the injector was less than 20°C, the producer rate was decreased; when the difference is above 35°C, the producer rate is increased; otherwise, the producer rate was kept constant.

5 RESULTS AND DISCUSSION

The simulations on the different upscaled grids allowed:

– to assess the impact of heterogeneities on the steam chamber developement, and on the oil production;

– to evaluate the impact of upscaling on the heterogeneity distribution.

5.1 Impact of Upscaling on Heterogeneity Distribution and Steam Chamber Growth

An important issue in upscaling, besides the choice of an appropriate technique, is the optimal level of coarsening. In the present case, the grids were upscaled in the only well direction only (*X* direction), to allow a better description of the steam chamber development around the injection well and a better heterogeneity distribution description in the coarser models. The optimum level of upscaling is then determined using both visual and quantitative analysis.

A comparaison of the litho-facies distribution and the steam chamber growth after 2 000 days of production for different upscaling factors is shown in Figure 12.

For an upscaling factor of 0.5 (upscaling × 2), the chamber is very similar to the fine reference model. If the upscaling factor is greater (*UF* = 0.2 or 0.1), the results are very different

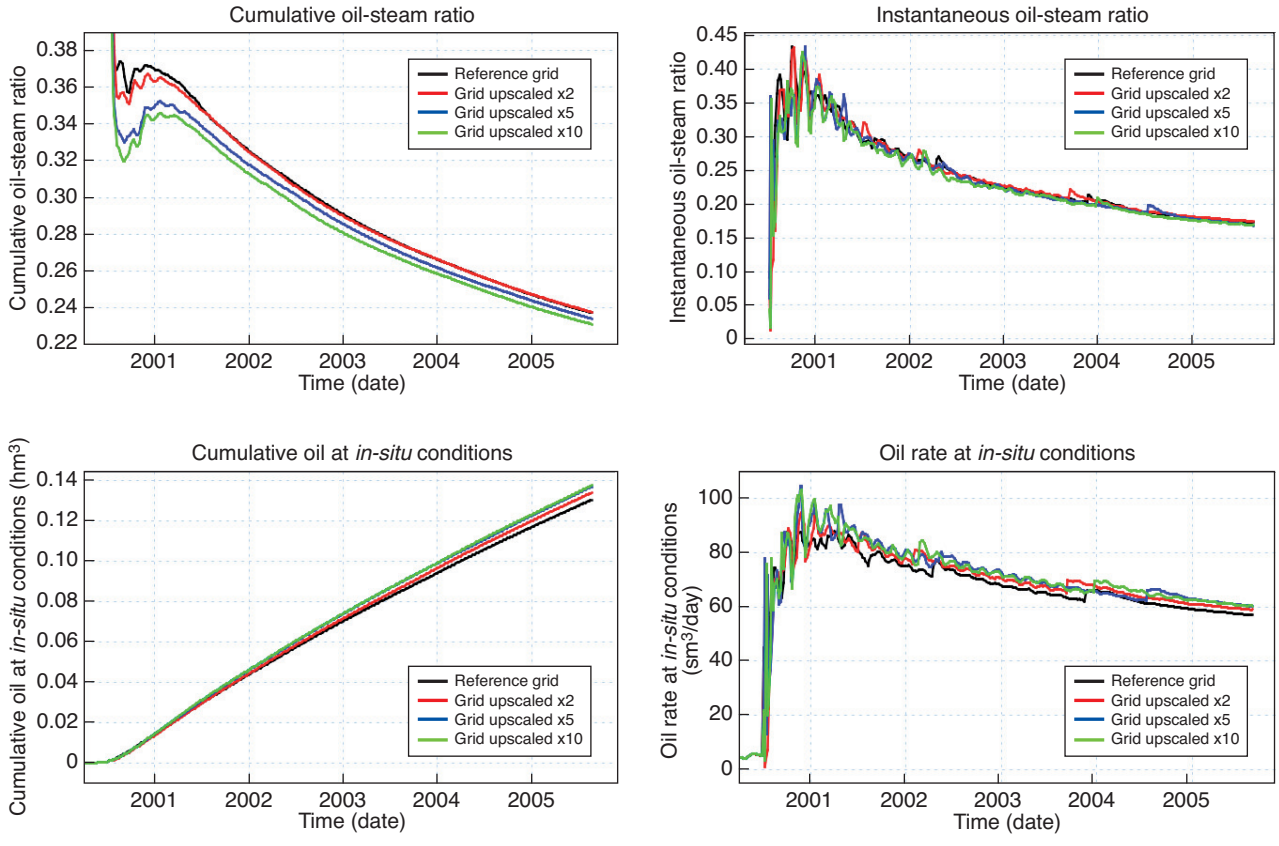

Figure 13

Cumulative and instantaneous oil-steam ratio, cumulative oil production and oil rate curves through time for the different upscaled models; for the reference model.

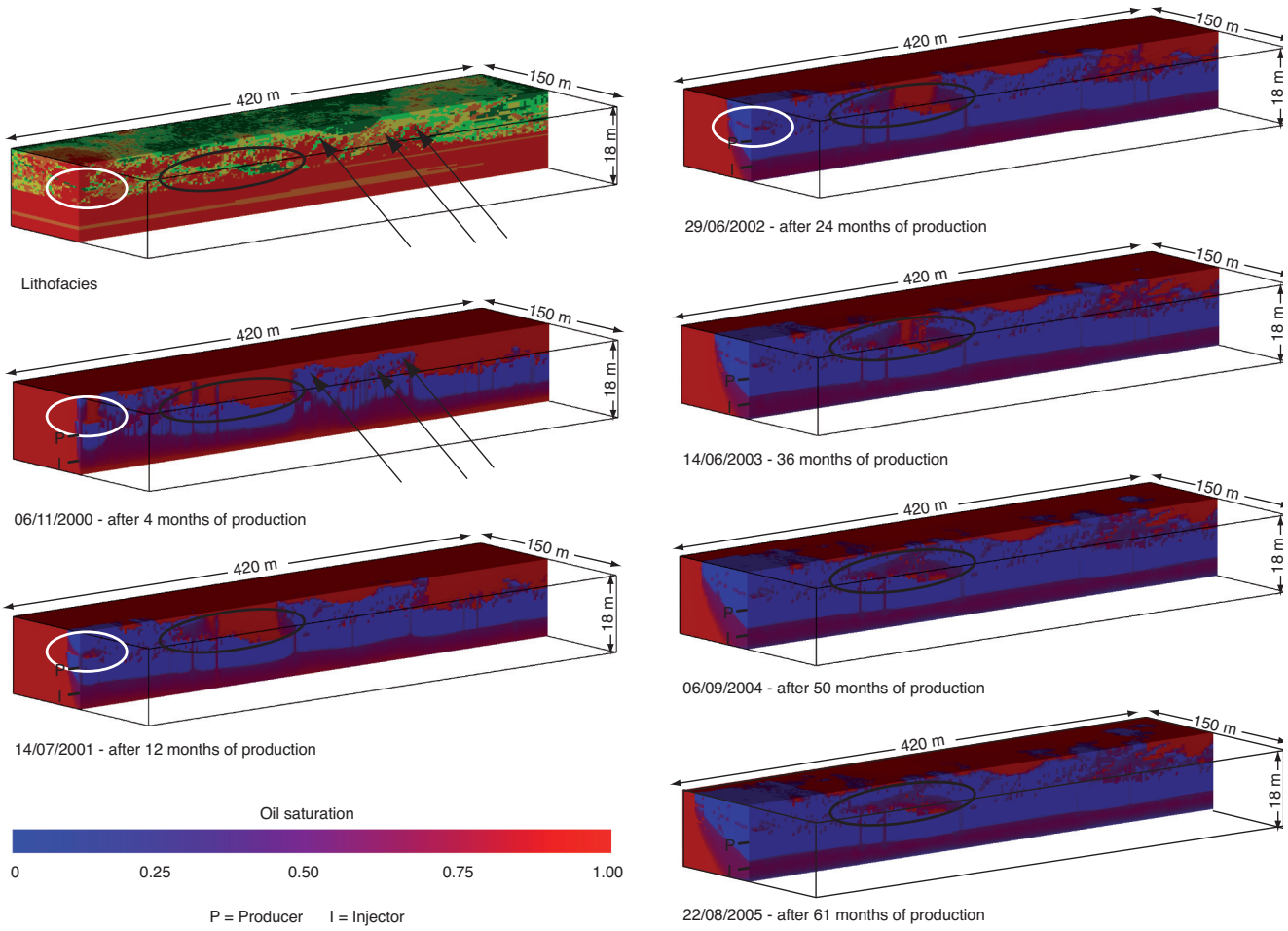

Figure 14

Oil saturation evolution in the reference model during production.

from the reference results: the heterogeneities are degraded. For an upscaling factor of 0.2, we can still observe the "large-scale" of heterogeneities but for $UF = 0.1$, even the "large-scale" heterogeneities (*e.g.* channel plugs) are significantly smoothed.

Even if the upscaling process smoothes the heterogeneities and influences the steam chamber growth, the field and the well results, oil-steam ratio and oil rate are quite similar, for every upscaling factor. As shown in Figure 13, the cumulative oil-steam ratio decreases over time for each considered upscaling factor and each curve tends to a similar value. Nevertheless, the cumulative oil-steam ratio is under-estimated in the early stage of production and for high upscaling factors. According to the curve displayed in Figure 13, the cumulative oil at the well is over-evaluated as the upscaling factor increases.

For an uspcaling factor of 0.1, we notice that the results in term of cumulative oil-steam ratio and cumulative oil are slightly closer to the reference than for $UF = 0.2$. This behaviour can be explained by an analysis of the upscaling process. The upscaling process combines two steps; the homogeneisation of the properties and a coarsening of the mesh. These two steps induce two types of error: an error due to homogeneization and an error due to the coarsening. The total error induced by an upscaling process is a non-intuitive combinaison of both of the effects (Sablok and Aziz, 2005) and the variation of the results depending on the upscaling extend is not monotonic. As shown in Figure 13, the instantaneous oil-steam ratio and oil rate seem to be irregular. This behaviour comes from the the combined effect of the high level of reservoir heterogeneity and the automated well behaviour. The steam chamber development is disturbed by the reservoir heterogeneities and that leads to a continuous modification of the well rates.

5.2 Effect of Heterogeneities

The fine grid (cell dimensions $2 \times 2 \times 0.25$ m) is used as the reference model for the heterogeneity effect assessment on the steam chamber development and oil production. This fine grid resolution allows us to describe accuratly the facies distribution and the steam chamber growth. Looking at the thermal simulation results, we can clearly see that the different heterogeneity types present in the meander belt have several degrees of impact on steam chamber development.

The large-scale heterogeneities (*e.g.* channel plug deposits) have a strong influence on the steam chamber development and therefore on fluid flow, all along the production process. Smaller scale heterogeneities (*e.g.* shale draping on the inclined sttratification) also influence steam flow in the reservoir but their effect is local and time-limited.

Figure 14 represents the oil saturation evolution in the reservoir during production. From these SAGD simulation results, the effect of heterogeneities on fluid flow is observable:

- the "small-scale" heterogeneities (*e.g.* shale draping) have an effect very early at the beginning of the steam injection (see *Fig. 14*, white circle) and in the production phase. Their influence is even stronger in the wellbore vicinity. After 12 months of production, the effect of these heterogeneities is attenuated, because steam and oil make their way around the shale drapes after the first months of injection. Nevertheless, it is difficult to observe the effect of the shale drapes with a thickness close to the limit of the resolution model on the simulation display (arrows in *Fig. 14*). However, at an early stage of the production (24 months, circle in *Fig. 14*), the cumulative oil-steam ratio curves for upscaled models are below the reference curve: the lower the upscaling factor, the lower the oil-steam ratio. The cumulative oil-steam ratio is under-estimated in the early stages of production and for high upscaling factors. This may be due to the fact that as we increased the upscaling, the "small scale" heterogeneities disappeared and the oil-steam ratio is lower than for models with small scale heterogeneities present. Later on in the production process, the oil-steam ratio curves tend to the same values whatever the upscaling factor. The impact of "small-scale" heterogeneities decreases through out the production process, as they are by-passed;
- the large-scale heterogeneities (*e.g.* channel plugs) strongly affect steam flow and oil production, during the whole production process. The channel plugs form large permeability barriers that prevent a good drainage efficiency of the reservoir. The channel plugs that we obseve in Figure 14 (see black circle) act as continuous barriers that compartimentalize the reservoir. In this example, the channel plugs are by-passed after three years of production.

CONCLUSIONS

The main objective of this study was to describe the impact of the point bar heterogeneities (small and large-scale heterogeneities) on the thermal recovery in heavy oil/bitumen production, for different upscaled models. As shown by the simulation results, the different scales of heterogeneities have a different impact on thermal recovery:

- small-scale heterogeneities corresponding to the shale draping in the inclined stratifications (IHS) have an impact on fluid flow at early stages (around 16 months) of steam injection. We observe that the temperature field and the steam saturation are not homogeneous in the reservoir corresponding to point bar deposits (red and orange lithofacies). At the same stage of injectioning, the oil was almost completely swept and produced in the reservoir part in the production well vicinity, as the oil saturation reaches almost zero in the point bar deposits. Small-scale heterogeneities impact steam injection and oil recovery very early in the production process. However, heterogeneities can be by-passed through time *via* 3-D paths in the reservoir;
- the large-scale heterogeneities, corresponding to channel plugs filled by silty shales and oxbow lake deposits, constitute real barriers for fluid flow (steam and oil). These impermeable barriers may be continuous at the reservoir scale and may prevent an efficient drainage of the reservoir, through out the production process;
- these results do not integrate the geomechanical effects during production, as no coupling was set between fluid-flow and mechanical modeling softwares;
- the upscaling effect on the well and field results is, on the whole, small;
- we must notice that the model has just one fractionnal flow curve and that a single porosity and permeability value have been deterministically attributed for each facies. A perspective would be to consider a more realistic statistical distribution of petrophysical properties, which would modify the results of upscaling;
- even if the well production obtained with the considered upscaling factors is close to the reference model results, the use of a fine description of reservoir heterogeneities is crucial and has to be taken into account during the early stage of production;
- only the reference model and upscaled models with small Upscaling Factors ($UF = 0.5$) preserve the small-scale heterogeneities and provide a good description of the steam chamber shape.

ACKNOWLEDGMENTS

The authors would like to thank Brigitte Doligez, Gérard Renard and Rémi Eschard from IFP Energies nouvelles for the valuable discussions and sharing their knowledge. The authors would like to also thank Eric Delamaide and Guy

Desaubliaux who reviewed this paper, providing helpful comments to improve the manuscript.

REFERENCES

Alexander J. (1992) Nature and origin of a laterally extensive alluvial sandstone body in the Middle Jurassic Scalby Formation, *J. Geol. Soc. London* **149**, 431-441.

Barton M.D. (1994) Outcrop characterization of architecture and permeability structure in fluvial-deltaic sandstones, Cretaceous Ferron sandstone, Utah, *PhD Dissertation*, University of Texas, Austin, Texas, 260 p.

Begg S.H., King P.R. (1985) Modeling the effect of shales on reservoir performance: Calculation of effective vertical permeability, *SPE Paper* 13529, 15 p.

Beucher H., Galli A., Le Loc'h G., Ravenne C., Heresim Group. (1993) Including a regional trend in reservoir modelling using the truncated Gaussian method, in *Geostatistics Tróia '92*, *Vol. 1*, Soares A. (ed.), Kluwer, Dordrecht, pp. 555-566.

Birrell G.E., Putnam P.E. (2000) A study of the influence of reservoir architecture on SAGD steam chamber development at the underground test facility, northeaster Alberta, Canada, using a graphical analysis of temperature profiles, *SPE Paper* 2000-104, *Canadian International Petroleum Conference (CIPC)*, Calgary, Canada, 8 June.

Cardwell W.T., Parsons R.L. (1945) Average permeabilities of heterogeneous oil sands, *Trans. AIME* **160**, 34-42.

Chen Q., Gerristen M.G., Kovscek A.R. (2007) Effect of reservoir heterogeneities on the steam-assisted gravity drainage process, *SPE ATCE 2007*, Anaheim, CA, USA, 11-14 November.

Crerar E.E., Arnott R.W.C. (2007) Facies Distribution and Stratigraphic Architecture of the Lower Cretaceous McMurray Formation, Lewis Property, Northeastern Alberta, *Bull. Can. Pet. Geol.* **55**, 99-124.

Doligez B., Beucher H., Geffroy F., Eschard R. (1999) Integrated reservoir characterization: improvement in heterogeneous stochastic modeling by integration of additional external constraints, in *Reservoir Characterization Recent Advances*, Schatzinger R., Jordan J. (eds), *AAPG Memoir* **71**, 333-342.

Doligez B., Beucher H., Lerat O., Souza O. (2007) Use of a seismic derived constraint: Different steps and joined uncertainties in the construction of a realistic geological model, *Oil Gas Sci. Technol.* **62**, 2, 237-248.

Durlofsky L.J. (2003) Upscaling of Geocellular Models for Reservoir Flow Simulation: A Review of Recent Progress, Paper presented at *7th International Forum on Reservoir Simulation*, Bühl/Baden-Baden, Germany, 23-27 June.

Eschard R., Houel P., Knox R., Ravenne C., Group HERESIM (1991) Three dimensional reservoir architecture of a valley-fill sequence and a deltaic aggradational sequence: influence of minor relative sea-level variations (Scalby Formation, England), *SEPM Concept in Sedimentology and Paleontology* **3**, 133-147.

Eschard R., Doligez B., Beucher H. (2002) Using quantitative outcrop databases as a guide for geological reservoir modelling, in *Geostatistics Rio 2000*, Armstrong M. *et al.* (eds), Ed. Kluwer Academic Publishers, pp. 7-17.

Farouq-Ali S.M. (1997) Is there life after SAGD? *J. Can. Pet. Technol.* **36**, 6, 20-23.

Flach P., Mossop G.D. (1985) Depositional Environments of Lower Cretaceous McMurray Formation, Athabasca Oil Sands, Alberta, *AAPG Bull.* **69**, 1195-1207.

Galli A., Beucher H., LeLoc'h G., Doligez B. (1994) The pros and cons of the truncated Gaussian method, in *Geostatistical Simulations*, Armstrong M., Dowd P.A. (eds), Kluwer Academic Publishers, Dordrecht, The Netherlands, pp. 217-233.

Galli A., Le Loc'h G., Geffroy F., Eschard R. (2006) An application of the truncated pluri-gaussian method for modeling geology, in *Stochastic modeling and geostatistics: principles, methods and case studies*, *AAPG Computer Applications in Geology* **5**, 2, 109-122.

Hartkamp-Bakker C.A., Donselaar M.E. (1993) Permeability patterns in point bar deposits: Tertiary Loranca Basin, central Spain, in *The geological modelling of hydrocarbon reservoirs and outcrop analogs*, Flint S.S., Bryant I.D. (eds), *Int. Association of Sedimentologists Special Publication*, *IAS* **SP15**, 157-168.

Jackson R.G. (1977) Preliminary evaluation of lithofacies models for meandering alluvial streams, in *Fluvial sedimentology*, Miall A.D. (ed.), *Can. Soc. Pet. Geol. Memoir* **5**, 543-576.

Jackson M.D., Muggeridge A.H. (2000) The effects of discontinuous shales on reservoir performance during horizontal waterflooding, *SPE J.* **5**, 446-455.

Joseph P., Rabineau M., Eschard R., Benard F. (1995) Quantification from satellite imaging of the sedimentary body geometry and facies distribution in the Senegal valley, *17th Regional Meeting Sedimentology (IAS) / 5e Congrès Français de Sédimentologie (ASF)*, Aix-les-Bains, 24-26 avril, Publication ASF n° **22**, p. 83.

Joshi S.D., Threlkeld C.B. (1985) Laboratory studies of thermally aided gravity drainage using horizontal wells, *AOSTRA J. Res.* **2**, 1, 11-19.

Le Loch G., Galli A. (1996) Truncated plurigaussian method: theoritical and practical point of view, in *Geostatistics Wollongong' 96, Vol. 1*, Baafi E.Y., Schofield N.A. (eds), Kluwer Academic Publisher, pp. 211-222.

Lemouzy P.M., Romeu R.K., Morelon I.F. (1993) A New Scaling-Up Method to Compute Relative Permeability and Capillary Pressure for Simulation of Heterogeneous Reservoirs, *SPE Paper* 26660, presented at the *SPE Annual Technical Conference and Exhibition*, Houston, 3-6 October.

Lerat O., Adjemian F., Baroni A., Etienne G., Renard G., Bathellier E., Forgues E., Aubin F., Euzen T. (2010) Modelling of 4D Seismic Data for the Monitoring of the Steam Chamber Growth During SAGD Process, *J. Can. Pet. Technol.* **49**, 6, 21-30. SPE-138401-PA.

Miall A.D. (1988) Reservoir heterogeneities in fluvial sandstones: Lessons from outcrop studies, *AAPG Bull.* **72**, 6, 682- 697.

Musial G., Reynaud J.Y., Gingras M.K., Féniès H., Labourdette R., Parize O. (2011) Subsurface and outcrop characterisation of large tidally influenced point bars of the Cretaceous Mc Murray Formation, Alberta, Canada, Accepted in *Sedimentary Geology*, April 2011.

Pemberton S.G., Flach P.D., Mossop G.D. (1982) Trace fossils from the Athabasca Oil Sands, Alberta, Canada, *Science* **217**, 825-827.

Preux C. (2011) Study of evaluation criteria for reservoir upscaling, Paper presented at the *73rd EAGE Conference & Exhibition Incorporating SPE EUROPEC 2011*, Vienna, Austria, 23-26 May.

Qi D., Hesketh T. (2004) Quantitative Evaluation of Information Loss in Reservoir Upscaling, *Pet. Sci. Technol.* **22**, 11, 1625-1640.

Renard P., de Marsily G. (1997) Calculating equivalent permeability: a review, *Adv. Water Resour.* **20**, 5-6, 253-278.

Richardson J.G., Harris D.G., Rossen R.H., Van Hee G. (1978) The effect of small, discontinuous shales on oil recovery, *J. Pet. Technol.* **20**, 1531-1537.

Robinson B., Kenny J., Hernandez-Hdez I.L., Bernal A., Chelak R. (2005) Geostatistical modeling integral to effective design and evaluation of SAGD processes of an Athabasca oilsands reservoir, a case study, *SPE/PS-CIM/CHOA International Thermal Operations and Heavy Oil Symposium*, Calgary, Alberta, Canada, 1-3 November, *SPE Paper* 97743.

Sablok R., Aziz K. (2005) Upscaling and discretization errors in reservoir simulation, *SPE Reservoir Simulation Symposium*, Houston, Texas, USA, 31 January-2 February, *SPE Paper* 93372.

Sharp J.M., Mingjuan Shi, Galloway W.E. (2003) Heterogeneity of fluvial systems – control on density-driven flow and transport, *Environ. Eng. Geosci.* **9**, 1, 5-17.

Smith D.G. (1988) Tidal bundles and mud couplets in the McMurray Formation, northeastern Alberta, Canada, *Bull. Can. Pet. Geol.* **36**, 216-219.

Smith D.G., Hubbard S.M., Leckie D.A., Fustic M. (2009) Counter point bar deposits: lithofacies and reservoir significance in the meandering modern Peace River and ancient McMurray Formation, Alberta, Canada, *Sedimentology* **56**, 1655-1669.

Swanson D.C. (1993) The importance of fluvial processes and related reservoir deposits, *J. Pet. Technol.* **45**, 368-377.

Willis B.J. (1989) Palaeochannel reconstructions from point bar deposits: A three-dimensional perspective, *Sedimentology* **36**, 757-766.

Willis B.J., White C.D. (2000) Quantitative outcrop data for flow simulation, *J. Sediment. Res.* **70**, 4, 788-802.

Willis B.J., Tang, H. (2010) Three-dimensional connectivity of point-bar deposits, *J. Sediment. Res.* **80**, 440-454.

Yang G., Butler R.M. (1992) Effects of reservoir heterogeneities on heavy oil recovery by steam assisted gravity drainage, *J. Can. Pet. Technol.* **31**, 8, 37-43.

Zhang W., Youn S., Doan Q. (2005) Understanding reservoir architectures and steam chamber growth at Christina Lake, Alberta, by using 4D seismic and Croswell seismis imaging, *SPE 97808*, November.

Zhang W., Youn S., Doan Q. (2007) Understanding reservoir architectures and steam-chamber growth at Christina Lake, Alberta, by using 4D seismic and crosswell seismic imaging, *SPE Reservoir Eval. Eng.* **10**, 5, 446-452. SPE-97808-PA.

Final manuscript received in May 2012
Published online in January 2013